



## Original Article

# Adequate taylor couette flow-mediated shear stress is useful for dissociating human iPSC cell-derived cell aggregates

Katsuhisa Matsuura<sup>a, b, \*, 1</sup>, Masanori Wada<sup>c, 1</sup>, Katsuhisa Sakaguchi<sup>d, 1</sup>,  
Yuki Matsuhashi<sup>e, 1</sup>, Tatsuya Shimizu<sup>a</sup>

<sup>a</sup> Institute of Advanced Biomedical Engineering and Science, Tokyo Women's Medical University, 8-1 Kawada-cho, Shinjuku, Tokyo, 162-8666, Japan

<sup>b</sup> Department of Cardiology, Tokyo Women's Medical University, 8-1 Kawada-cho, Shinjuku, Tokyo, 162-8666, Japan

<sup>c</sup> ABLE Corporation, 5-9 Nishigoken-cho, Shinjuku, Tokyo, 162-0812, Japan

<sup>d</sup> School of Creative Science and Engineering, TWIns, Waseda University, 2-2 Wakamatsu-cho, Shinjuku-ku, Tokyo 162-8480, Japan

<sup>e</sup> Graduate School of Advanced Science and Engineering, TWIns, Waseda University, 2-2 Wakamatsu-cho, Shinjuku-ku, Tokyo 162-8480, Japan



## ARTICLE INFO

## Article history:

Received 8 November 2018

Received in revised form

2 March 2019

Accepted 10 April 2019

## Keywords:

iPSC cell

3D suspension culture

Cell aggregate dissociation device

Taylor couette flow

## ABSTRACT

Pluripotent stem cell including induced pluripotent stem cells (iPSC) are promising cell sources for regenerative medicine and for three-dimensional suspension culture technologies which may enable the generation of robust numbers of desired cells through cell aggregation. Although manual procedure is widely used for dissociating cell aggregates, the development of non-manual procedures using devices will contribute to efficient cell manufacturing. In the present study, we developed novel cell aggregate dissociation devices with a rotating cylinder inside based on Taylor Couette flow-mediated shear stress. The shear stress can be increased according to an increase in the size of the rotating cylinder inside the devices and the rotation rate. Adequate device size and suitable rotation rate efficiently dissociated cell aggregates after the undifferentiated expansion and the cardiac differentiation of human iPSC. These findings suggest that non-manual device procedure might be useful for harvesting single cells from human iPSC-derived cell aggregates.

© 2019, The Japanese Society for Regenerative Medicine. Production and hosting by Elsevier B.V. This is an open access article under the CC BY-NC-ND license (<http://creativecommons.org/licenses/by-nc-nd/4.0/>).

## 1. Introduction

Pluripotent stem cells (PSC) including induced pluripotent stem cells (iPSC) are promising cell sources for generating desired cells for cell and tissue transplantation. Numerous numbers of cells are estimated to be necessary for regenerative medicine in the heart and the pancreas, and a scalable cell production system is a fundamental technology for the realization of various types of regenerative medicine in particular using allogeneic PSC. Recent advancement of three-dimensional (3D) suspension culture technologies has enabled the generation of robust numbers of not only undifferentiated iPSC [1], but also iPSC-derived cardiomyocyte [2],

vascular endothelial cell [3], pancreatic progenitor cell/islet [4,5], thyroid follicular cell [6] and megakaryocyte [7]. The produced cells have also been reported to function in vitro and in vivo through integration with tissue engineering technologies [8–12]. However, there are still some issues to be resolved in cell manufacturing processes, in particular, the process after the cell production. Although 3D suspension culture strategies generate desired cells through cell aggregation, the dissociation to single cells is an indispensable step for use in not only transplantation and tissue fabrication, but also cell quality evaluation through cell number counting, flow cytometric analysis and single cell analysis. Currently the dissociation process of cell aggregates is widely performed by manual procedure with pipetting. Scale up of culture vessels and the advancement of automated culture medium exchange systems will produce larger numbers of cells and cell aggregates. Therefore, manual cell aggregate dissociation strategies will not be applicable in terms of operation time needed. However, the cell aggregates dissociation strategies without manual procedure have not been developed yet. Furthermore, the adequate

\* Corresponding author. Institute of Advanced Biomedical Engineering and Science, Tokyo Women's Medical University, 8-1 Kawada-cho, Shinjuku, Tokyo, 162-8666, Japan. Fax: +81 3 3359 6046.

E-mail address: [matsuura.katsuhisa@twmu.ac.jp](mailto:matsuura.katsuhisa@twmu.ac.jp) (K. Matsuura).

Peer review under responsibility of the Japanese Society for Regenerative Medicine.

<sup>1</sup> These authors equally contributed to this work.

shear stress levels for cell aggregate dissociation to single cells remain elusive. Various types of impellers are used to agitate cells in 3D suspension culture and they might be applicable to dissociate cell aggregates through the increase of shear stress according to the increase of agitation rate. But since the frequent collision of cells with impellers will lead to cell death, the device without impellers might be suitable regarding the cell harvest efficiency.

In this study, we present a novel cell aggregate dissociation device based on the Taylor Couette flow-mediated shear stress. Taylor Couette flow is a vortex flow generated between the cylinders in a system in which the outer cylinder is stationary and the inner cylinder rotates between the concentric double cylinders. This newly type of device enabled to generate shear stress without using impellers and the efficient dissociation of cell aggregates after the undifferentiated expansion and the cardiac differentiation of human iPSC.

## 2. Materials and methods

### 2.1. Antibodies and reagents

The following antibodies were used for immunocytochemistry and flow cytometric analysis: anti-cardiac troponin T (cTnT) mouse monoclonal antibody (Thermo Scientific, Rockford, IL, USA), anti-cTnT rabbit polyclonal antibody (Abcam, Cambridge, UK), FITC-conjugated anti-SSEA-4 mouse monoclonal antibody (R&D systems, Minneapolis, MN, USA) and FITC-conjugated anti-Tra-1 60 mouse monoclonal antibody (BD Biosciences, San Jose, CA, USA). Anti-mouse IgG<sub>1</sub> (Agilent, Santa Clara, CA, USA) and FITC-conjugated anti-mouse IgG<sub>3</sub> (R&D systems) and anti-mouse IgMκ (BD Biosciences) isotype control antibodies were used for negative control. Secondary antibodies were purchased from Jackson ImmunoResearch Laboratories (West Grove, PA, USA).

### 2.2. Visualization of Taylor Couette flow using particle imaging velocimetry

The Taylor Couette flow in the cell separation vessel was visualized using fluorescent particle imaging velocimetry (PIV) as described previously [13]. The cell separation vessel was made of silicone (KE-1603, Shin-Etsu Chemical, Tokyo, Japan) in order to match the refractive index with that of working fluid as 1.4096. The solution containing the fluorescent particles (FLUOSTAR, EBM Co., Ltd, Tokyo, Japan) was filled in the cell separation vessel, and the refractive index was adjusted to that of the silicone vessel using glycerin. An Nd:YAG laser beam (DS20-527, Photonics Industries, Bohemia, NY, USA) was used to irradiate the particles in the vessel. The PIV images were taken using a high-speed camera (VC13-0192, Imager Pro XL, LaVision, Goettingen, Germany) through an optical filter with a cutoff frequency of 550 nm (CVI Melles Griot, Albuquerque, NM, USA). Pixel size was 0.025 mm and frame speed was 400 frames/s. The imaging analysis was performed using Davis 8.2.2 software (LaVision).

### 2.3. Human iPSC culture

Human iPSC line Ff-I14 (iPSC stock for non-clinical use) was provided by the Center for iPSC Cell Research and Application, Kyoto University. 771-2 human iPSC line was purchased from Reprocell (Yokohama, Japan). iPSC were maintained on iMatrix511 (Nippi, Tokyo, Japan) in StemFit AK03N (Ajinomoto, Tokyo, Japan). Cells were passaged as single cells every 7–8 days using TrypLE Select (Life Technologies, Carlsbad, CA, USA) as described elsewhere [14].

### 2.4. 3D suspension culture for undifferentiated expansion

Human iPSC cultured on iMatrix511 were dissociated with TrypLE Select and a single cell suspension ( $1.5 \times 10^5$  cells/mL for 771-2,  $2.0 \times 10^5$  cells/mL for Ff-I14) was cultured in StemFit AK03N medium with Y27632 (10  $\mu$ M) (Wako, Tokyo, Japan) in a 100 mL stirred bioreactor system (Bio Jr. 8; ABLE Co., Tokyo, Japan) until day 4. The agitation rates were 40 rpm. Dissolved oxygen was maintained at 40% with air, oxygen or nitrogen. pH was maintained at 7.2 by CO<sub>2</sub> addition, and the temperature was maintained at 37 °C for the entire process. At day 2 and day 3, the culture medium was exchanged.

### 2.5. 3D suspension culture for cardiac differentiation

Human iPSC (Ff-I14) cultured on iMatrix511 were dissociated with TrypLE Select and a single cell suspension was cultured on EZSPHERE (10 cm diameter) (AGC Techno Glass, Shizuoka, Japan) for 4 days in StemFit AK03N medium not containing component C with Y27632 (10  $\mu$ M) at 37 °C in humid air with 5% CO<sub>2</sub> and 1% O<sub>2</sub>. At day 4, cell aggregates were collected from EZSPHERE dishes and resuspended in StemFit AK03N medium not containing component C and cultured in a 100 mL stirred bioreactor system (ABLE) until day 13 or 14. The following growth factors and small molecules were used at the corresponding days: days 0–1, 2 ng/mL BMP4 (R&D systems); days 1–4, 10 ng/mL BMP4, 6 ng/mL Activin A (R&D systems), 10 ng/mL bFGF (ReproCell); days 4–8, 1  $\mu$ M IWP-3 (Stemgent, Lexington, MA, USA), 0.6  $\mu$ M Dorsomorphine (Sigma–Aldrich, St. Louis, MO, USA), 5.4  $\mu$ M SB432542 (Sigma Aldrich); after day 8, 5 ng/mL VEGF (R&D Systems) and 10 ng/mL bFGF. At days 6, 8, 10, and 12, the culture medium was exchanged.

### 2.6. Cell aggregates dissociation

For the dissociation of cell aggregates after the undifferentiated expansion, cell aggregates in a 100 mL vessel were washed with PBS(–) once and assigned equally to the following 4 groups for dissociation. In manual procedure, cell aggregates were treated with 12.5 mL of TrypLE Select (1  $\times$  TrypLE Select for 771-2 and 0.5  $\times$  TrypLE Select for Ff-I14) for 5 min (Ff-I14) or 10 min (771-2) in waterbus at 37 °C and then dissociated with pipetting for 2 min. In device procedure, cell aggregates were dissociated with 12.5 mL of TrypLE Select (1  $\times$  TrypLE Select for 771-2 and 0.5  $\times$  TrypLE Select for Ff-I14) for 5 min (Ff-I14) or 10 min (771-2) in each device with a rotating cylinder inside of  $\Phi$ 22mm,  $\Phi$ 25mm or  $\Phi$ 28mm (Fig. 1 a, b). Devices were set on stirrers at 37 °C in humid air with 5% CO<sub>2</sub> and rotation rate of devices was 1200 rpm. After dissociation, cell number was calculated with trypan blue staining. Sample images were obtained by an inverted microscopy (Nikon, Tokyo, Japan) with NIS-Elements software (Nikon).

For the dissociation of cell aggregates after the cardiac differentiation, cell aggregates in 40 mL of 100 mL from a 100 mL vessel were washed with PBS(–) once and assigned equally to the following 2 groups for dissociation. In manual procedure, cell aggregates were treated with 12.5 mL of 0.05% trypsin/EDTA (Life Technologies) for 10 min in waterbus at 37 °C and then dissociated with pipetting for 2 min. In device procedure, cell aggregates were dissociated with 12.5 mL of 0.05% trypsin/EDTA for 10 min in a device with a rotating cylinder inside of  $\phi$ 28mm (Fig. 1 a, b). Devices were set on stirrers at 37 °C in humid air with 5% CO<sub>2</sub> and rotation rate of device was 1500 rpm. After dissociation, cell number was calculated with trypan blue staining and cells were cultured on 24 well plates (Corning, Corning, NY, USA) for several days in DMEM supplemented with 10% fetal bovine serum at 37 °C in a humidified atmosphere with 5% CO<sub>2</sub>.

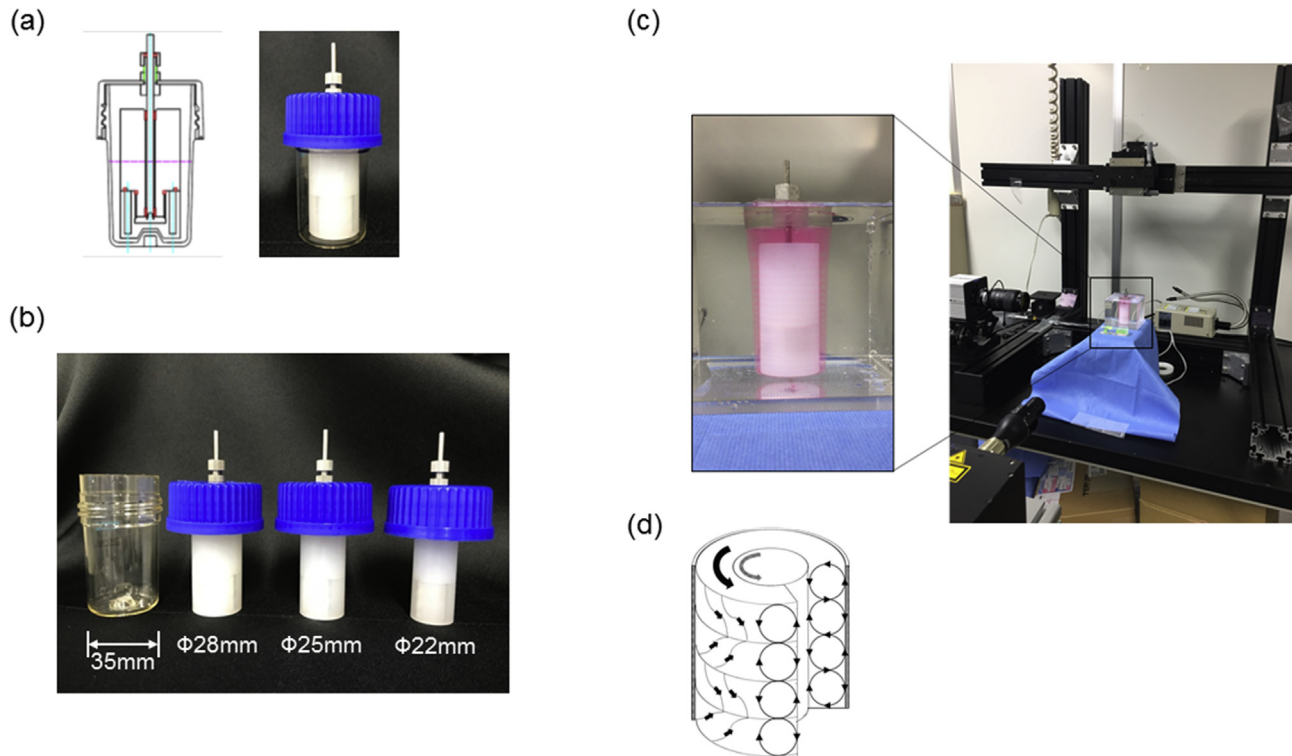


**Fig. 1.** Cell aggregate dissociating devices and PVI experiment apparatus. (a) Left, schematic illustration of the cell aggregate dissociation device. The photograph shows the device. (b) The photograph shows the devices with a rotating cylinder inside of  $\phi 22\text{mm}$ ,  $\phi 25\text{mm}$  or  $\phi 28\text{mm}$ . (c) PVI experiment apparatus. (d) Schematic illustration of the Taylor-Couette flow in the device.

### 2.7. Immunocytochemistry

Cells were fixed with 4% paraformaldehyde, and immunocytochemistry was performed as described previously [11]. Nuclei were stained with Hoechst 33,258 (Life Technologies). Samples were imaged by ImageXpress (Molecular Device, Sunnyvale, CA, USA) with MetaXpress and AcuityXpress software (Molecular Device).

### 2.8. Flow cytometric analysis

Cells were fixed with 4% paraformaldehyde, and were immunostained for flow cytometric analysis as described previously [1,11]. Stained cells were analysed using a Gallios (Beckman Coulter, Brea, CA, USA) and Kaluza software (Beckman Coulter).

### 2.9. RNA extraction and quantitative RT-PCR

Total RNA extraction and RT-PCR were performed as described previously [15]. Quantitative PCR was performed with a 7300 Real Time PCR System (Applied Biosystems, Foster City, CA, USA). Relative mRNA expression levels were calculated using a standard curve of GAPDH mRNA levels. All primers were obtained from Applied Biosystems (LIN28: Hs00702808\_s1, GAPDH: Hs00266705\_g1).

### 2.10. Statistical analysis

Data are presented as mean  $\pm$  standard deviation. Statistical analyses were performed with the Student's *t*-test for comparison between two groups. Multiple group comparisons were performed by one-way analysis of variance followed by Tukey–Kramer procedure for comparison of means. A value of  $p < 0.05$  was considered statistically significant.

## 3. Results

### 3.1. Taylor Couette flow analysis in cell aggregate dissociation devices

To dissociate cell aggregates through shear stress without using impellers, we developed a cell aggregate dissociation device with a rotating cylinder inside (Fig. 1a). Three types of devices with gaps of 3.5 mm ( $\phi 28$ ), 5 mm ( $\phi 25$ ) and 6.5 mm ( $\phi 22$ ) between the cylinder and the inner wall of the bottle were prepared from polypropylene with a cutting processing machine (Fig. 1b).

At first, we attempted to visualize the flow in those devices using the fluorescent particles (Fig. 1c). The PIV analysis of the flow in the cell separation vessel (Fig. 1c) showed that Taylor-Couette flow was observed at any cylinder size of 22 mm, 25 mm, and 28 mm in diameter, and at any rotation speed of 500 rpm, 1000 rpm, and 1500 rpm (Figs. 1d and 2, Supplementary Video 1–19). Furthermore, the shear stress generated by this analysis was measured. The shear stress increased according to the increase of rotation rates in every size of device (Fig. 3a) and they also increased according to the increase of cylinder size at every rotation rate (Fig. 3b). Importantly, significant strong physical force was estimated to be generated to the cell aggregate-mimicking particles in  $\phi 28\text{mm}$  device at both 1000 rpm and 1500 rpm. We also calculated Reynolds number based on the maximum velocity in each device according to the rotation rate (Fig. 3c). As shown in Fig. 3d, Reynolds number was increased according to the increase of the rotation rate in  $\phi 22\text{mm}$  device, while the maximum Reynolds number was observed at 1000 rpm in  $\phi 25\text{mm}$  and  $\phi 28\text{mm}$  devices.

Supplementary video related to this article can be found at <https://doi.org/10.1016/j.reth.2019.04.006>

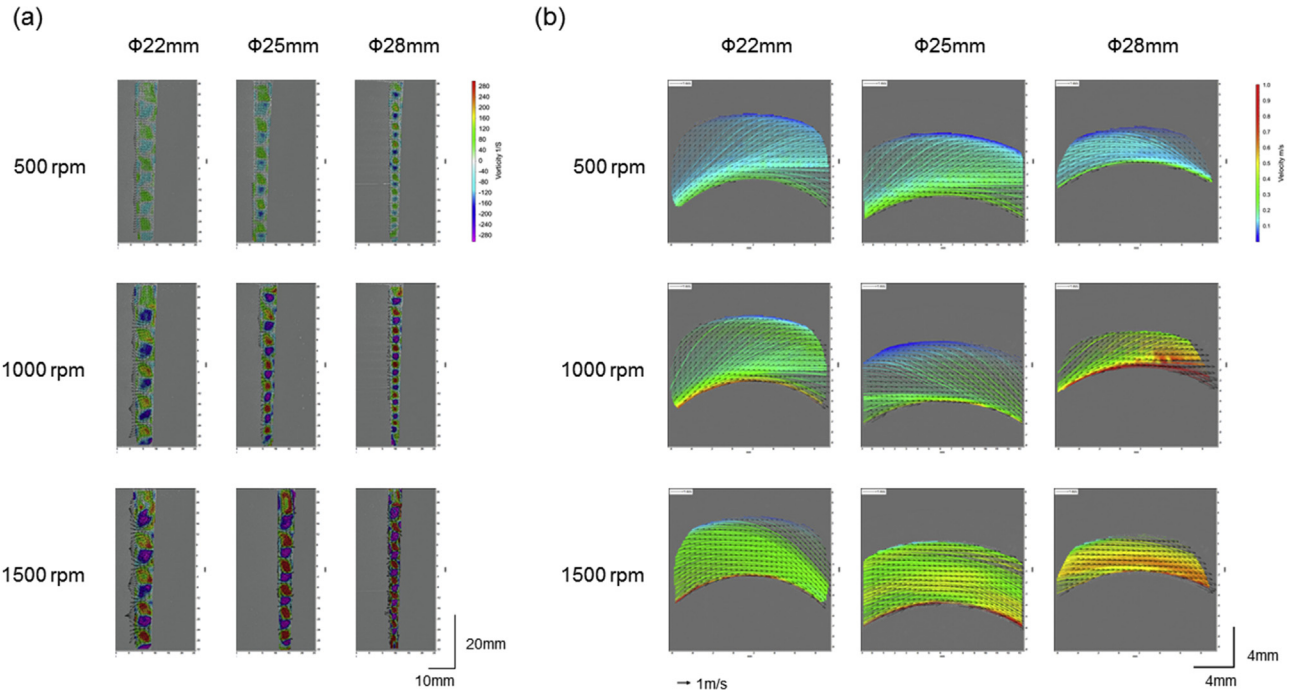


**Fig. 2.** Representative flow images in each size of devices and each rotation rate (a and b) Representative flow images from the lateral view (a) and upper view (b). Colors mean vorticity (a) and velocity (b).

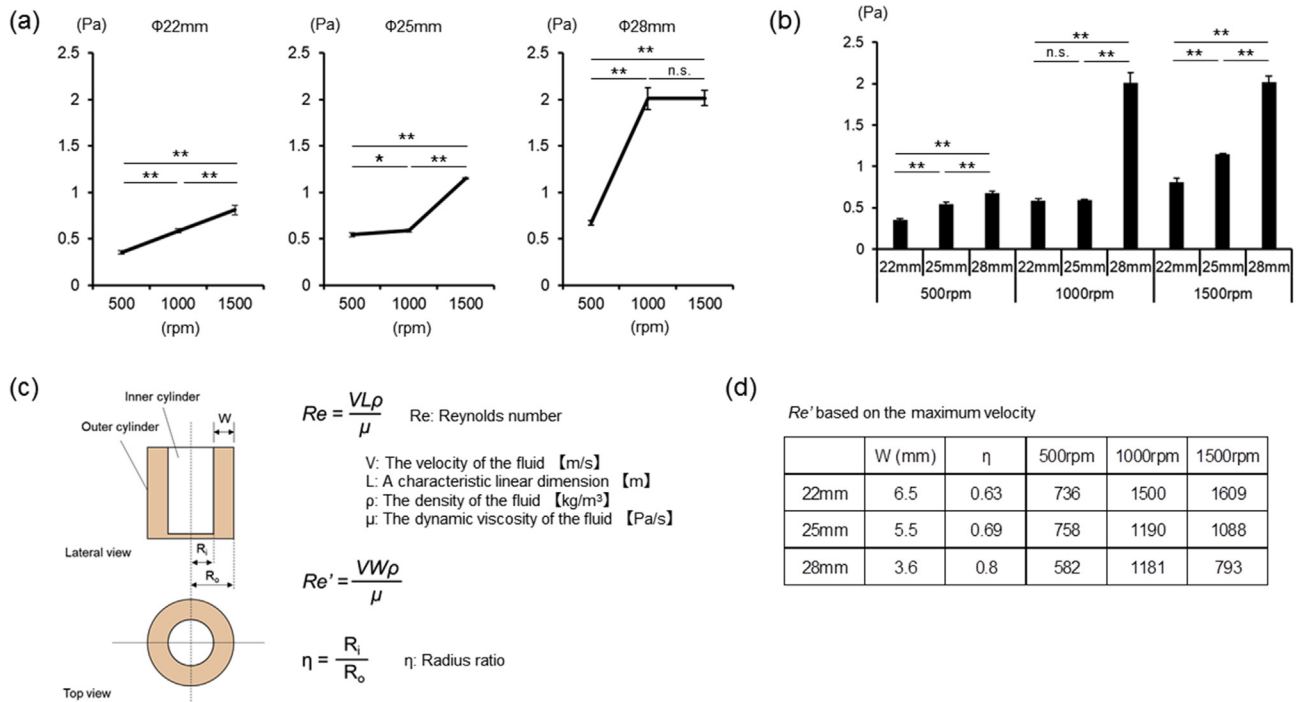


**Fig. 3.** Shear stress measurement using PVI experiment apparatus. Shear stress (Pa) according to the rotation rates in each size of device (a) and the size of devices in each rotation rates (b). n = 3. \*p < 0.05. \*\*p < 0.01. n. s., not significant. (c) The illustrated scheme for calculation of Reynolds number. (d) Reynolds number based on the maximum velocity.

### 3.2. Dissociation of undifferentiated cell aggregates using cell aggregation dissociation devices

Next we examined whether these devices dissociated cell aggregates from human iPSC. When a single cell suspension from feeder-free iPSC was inoculated in a 100 mL bioreactor, robust

numbers of cell aggregates were generated at day 4 (Fig. 4a). When cell aggregates from 771–2 and Ff-14 were dissociated with manual procedure, a single cell suspension was obtained and  $2.4 \pm 0.8 \times 10^7$  cells and  $4.9 \pm 1.5 \times 10^7$  cells were isolated, respectively (Fig. 4a and b). As these cell numbers were the results using 1/4 volume of a 100 mL vessel, total cell number in a 100 mL

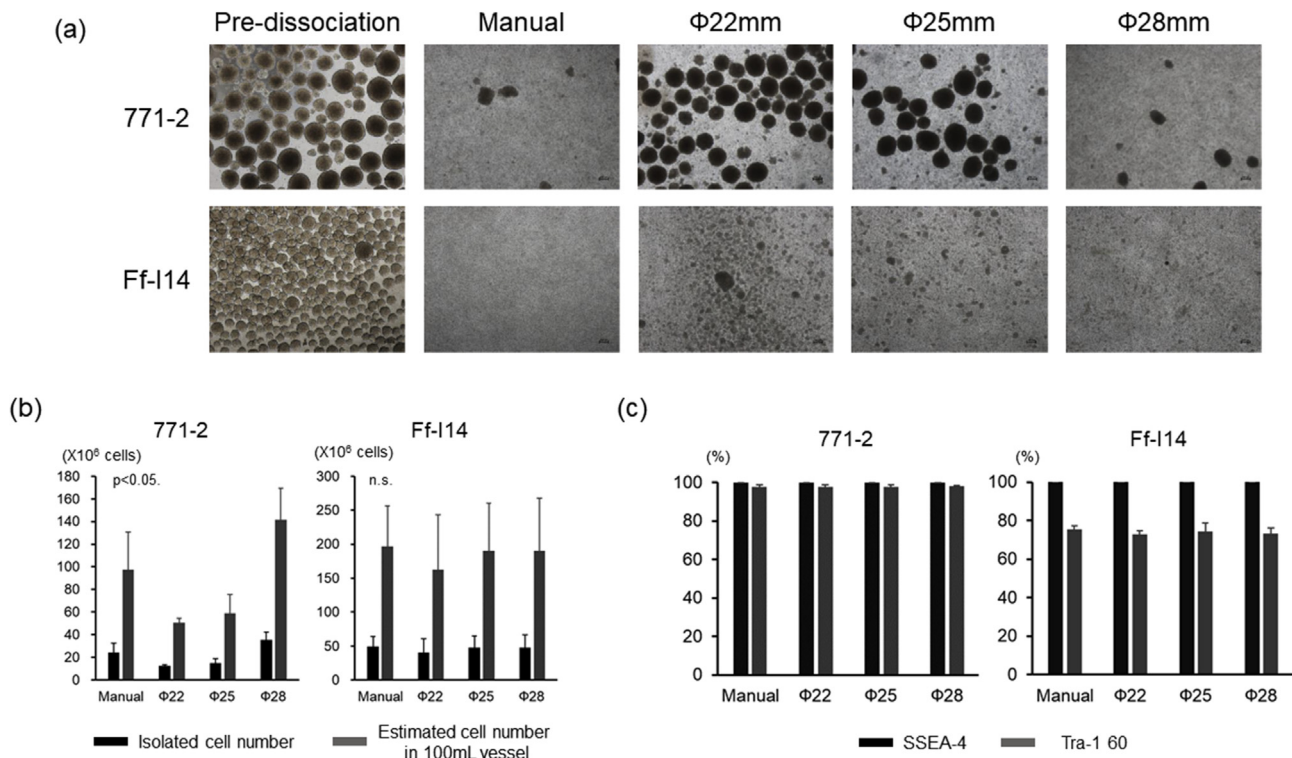


**Fig. 4.** Dissociation of human iPSC-derived cell aggregates after the undifferentiated expansion. (a) Four days after the expansion in a bioreactor, cell aggregates were dissociated with manual procedure or cell aggregate dissociation devices. Representative image of cells before and after the dissociation. Bars, 100  $\mu$ m. (b) Isolated cell number and estimated cell number in a 100 mL vessel ( $n = 3$ ). (c) Flow cytometric analysis of dissociated cells. The percentage of SSEA-4 and Tra-1 60 positive cells was calculated and shown in the graph ( $n = 3$ ).

vessel was estimated to be  $9.7 \pm 3.3 \times 10^7$  cells (771-2) and  $2.0 \pm 0.6 \times 10^8$  cells (Ff-I14), respectively (Fig. 4b). Flow cytometric analysis revealed that almost all of cells expressed SSEA-4 and many cells expressed Tra-1 60 (Fig. 4c). These findings suggest that 3D suspension culture efficiently expanded human iPSC while maintaining their undifferentiated status.

Then we compared the dissociation efficiency of undifferentiated cell aggregates between manual procedure and device procedure. When cell aggregates from 771-2 iPSC were dissociated with manual procedure and  $\phi 28$ mm device at 1200 rpm, there was small number of remaining cell aggregates (Fig. 4a) and the isolated cell number in the  $\phi 28$ mm device was approximately 1.4 times of that isolated in manual procedure (isolated cell number:  $3.5 \pm 0.7 \times 10^7$  cells, estimated cell number in a 100 mL vessel:  $1.4 \pm 0.3 \times 10^8$  cells, Fig. 4b). However, many cell aggregates remained after dissociation with  $\phi 22$ mm and  $\phi 25$ mm devices at 1200 rpm (Fig. 4a) and the isolated cell number in  $\phi 22$ mm and  $\phi 25$ mm devices was about 50% and 60% of that in manual procedure, respectively (isolated cell number:  $1.3 \pm 0.1 \times 10^7$  cells ( $\phi 22$ mm),  $1.5 \pm 0.4 \times 10^7$  cells ( $\phi 25$ mm), estimated cell number in a 100 mL vessel:  $5.0 \pm 0.4 \times 10^7$  cells ( $\phi 22$ mm),  $5.9 \pm 1.6 \times 10^7$  cells ( $\phi 25$ mm), Fig. 4b).

On the other hand, when cell aggregates from Ff-I14 iPSC were dissociated with manual procedure and device procedure at 1200 rpm, there were few large remaining cell aggregates except for the dissociation with  $\phi 22$ mm device (Fig. 4a). Isolated cell number in  $\phi 22$ mm device was about 80% of that in manual procedure (isolated cell number:  $4.1 \pm 2.0 \times 10^7$  cells, estimated cell number in a 100 mL vessel:  $1.6 \pm 0.8 \times 10^8$  cells, Fig. 4b), but the dissociation using  $\phi 25$ mm and  $\phi 28$ mm devices enabled the harvest of equivalent numbers of cells that by manual procedure (isolated cell number:  $4.8 \pm 1.8 \times 10^7$  cells ( $\phi 25$ mm),

$4.8 \pm 1.9 \times 10^7$  cells ( $\phi 28$ mm), estimated cell number in a 100 mL vessel:  $1.9 \pm 0.7 \times 10^8$  cells ( $\phi 25$ mm),  $1.9 \pm 0.8 \times 10^8$  cells ( $\phi 28$ mm), Fig. 4b). The percentage of SSEA-4 and Tra-1 60 expressing cells was identical between manual procedure and device procedures (Fig. 4c).

### 3.3. Dissociation of cell aggregates after the cardiac differentiation using cell aggregation dissociation device

Next we examined whether human iPSC-derived aggregates after the cardiac differentiation could be dissociated with the device procedure. When cell aggregates at 13 or 14 days of cardiac differentiation were dissociated with manual procedure,  $4.7 \pm 0.9 \times 10^7$  cells were isolated (Fig. 5a). As this cell number was the results using 1/5 volume of a 100 mL vessel,  $2.4 \pm 0.5 \times 10^8$  cells were estimated to be harvested in a 100 mL vessel (Fig. 5a). Flow cytometric analysis revealed that around 89% of cells were positive for cTnT (Fig. 5b and c), suggesting that  $2.1 \times 10^8$  cardiomyocytes might be generated in a single run. When cell aggregates in the same preparations were dissociated with the  $\phi 28$ mm device at 1500 rpm,  $4.7 \pm 0.3 \times 10^7$  cells were isolated, indicating that  $2.4 \pm 0.1 \times 10^8$  cells were estimated to be isolated in a 100 mL vessel (Fig. 5a). Flow cytometric analysis revealed that around 93% of cells were positive for cTnT (Fig. 5b and c), suggesting that  $2.2 \times 10^8$  cardiomyocytes might be generated in a single run. Herein, device procedure might be useful for isolating cardiomyocytes from cell aggregates similar to isolation by manual procedure.

To elucidate the influence on cardiomyocyte viability, we cultured same number of isolated cardiomyocytes from manual or device procedure for a couple of days and evaluated the number of cardiomyocyte by immunocytochemistry. As shown in Fig. 5d and e, the number of cTnT positive cardiomyocytes was identical

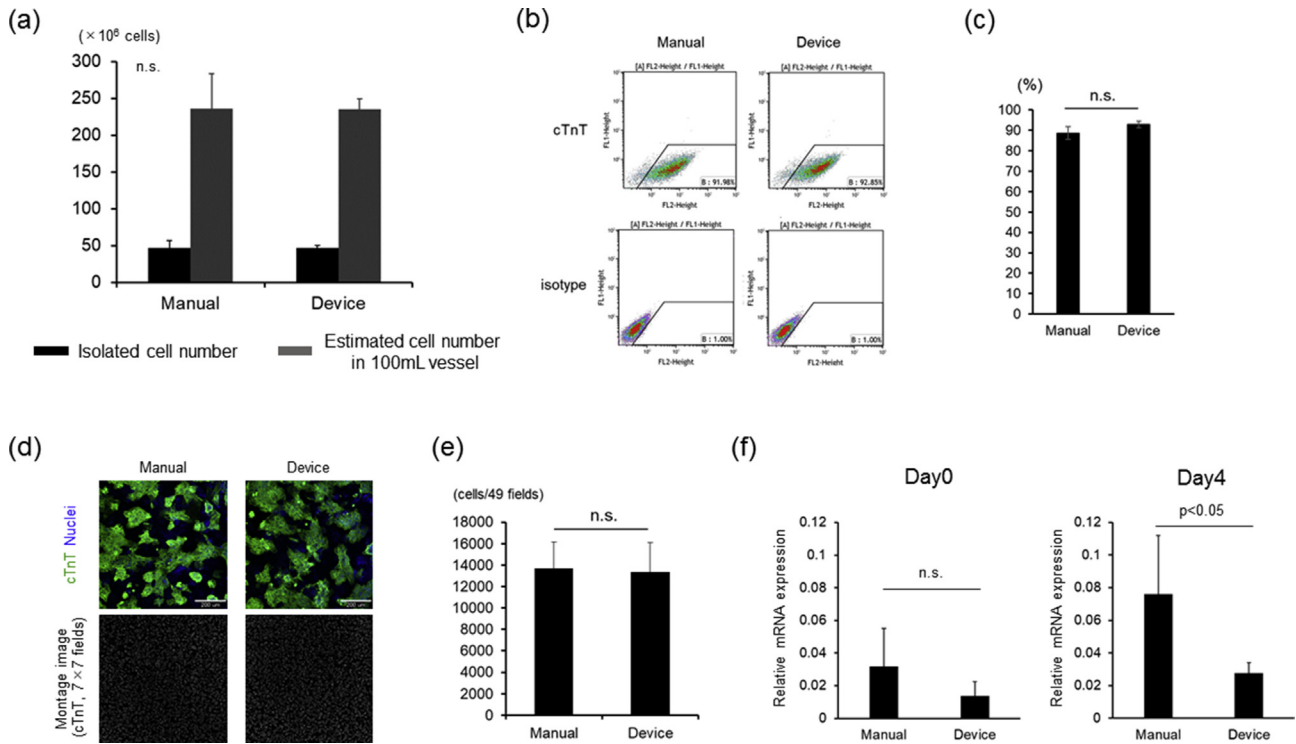


**Fig. 5.** Dissociation of human iPSC-derived aggregates after the cardiac differentiation. (a) The number of isolated cells according to the difference of dissociation methods ( $n = 4$ ). (b) Representative images of flow cytometric analysis to evaluate the percentage of cTnT positive cells in dissociated samples. (c) Percentage of cTnT positive cells in dissociated samples by flow cytometric analysis ( $n = 4$ ). n. s., not significant. (d) Representative images of cardiomyocytes (cTnT, green) 2 days after the cultivation. Nuclei were stained with Hoechst (blue). Bars, 200  $\mu\text{m}$ . Lower, montage images of 49 fields ( $7 \times 7$  fields) of cTnT stained images (original magnification of each field is  $\times 20$ ). (e) The number of cTnT positive cells. The number of cTnT positive cells in 49 fields ( $7 \times 7$  fields) for each sample were calculated and shown in the graph ( $n = 4$ ). n. s., not significant. (f) Lin 28 mRNA expression in human iPSC-derived cardiomyocytes. Lin28 mRNA expression levels in iPSC-derived cardiomyocytes just after the dissociation and at 4 days after dissociation ( $n = 4$ ). n. s., not significant.

between manual and device procedure, suggesting that device procedure might not affect cardiomyocyte viability.

Finally, we examined the influence of device procedure on the remaining undifferentiated iPSC after the cardiac differentiation. Although Tra-1 60 positive cells were not observed just after dissociation with manual and device procedure by flow cytometric analysis (data not shown), Lin 28 mRNA expression was slightly observed and the expression levels just after the dissociation were not different in both dissociation strategies (Fig. 5f). Interestingly when the dissociated cells were cultured for 4 days, Lin28 expression levels were significantly higher in cells after the manual procedure than that in cells after the device procedure (Fig. 5f). These findings indicate that device dissociation strategies might inhibit the growth of remaining iPSC.

#### 4. Discussion

In the present study, we developed novel cell aggregate dissociation devices for isolating human iPSC-derived cells. Taylor couette flow in the devices generated shear stress and contributed to the efficient dissociation of cell aggregates after the undifferentiated expansion and the cardiac differentiation.

A scalable cell production system is indispensable for the practical application of regenerative medicine and many researchers, including ourselves, have developed cell culture strategies to expand PSC and generate desired cells such as cardiomyocytes and pancreas islets using cell aggregate/embryoid body-based 3D suspension culture [2,5,16,17]. These upstream processes of cell manufacturing have been attractive for many researchers, because the development requires the collaboration of

engineers and stem cell scientists. Recently Nath et al. have reported that the treatment with botulinum hemagglutinin breaks up undifferentiated cell aggregates of human iPSC into small ones, which also enables the serial passaging and high density culture in a 3D suspension bioreactor without using enzymes [18]. On the other hand, the downstream processes including cell aggregate dissociation, cell dispensation, and cell freezing are also indispensable for practical application of regenerative medicine, but currently many researchers dissociate cell aggregates through manual procedures with pipetting. However, manual procedure is not applicable for robust numbers of cell aggregates in terms of operation time needed. Therefore, the development of cell aggregate dissociation strategies without manual procedure will be necessary. The devices in the present study generated shear stress through Taylor Couette flow without using impellers and there are few reports on the application of Taylor Couette flow for PSC culture. In the case of dissociation of 771–2 cell aggregates, the isolated cell number in a  $\phi 28\text{mm}$  device was around 1.4 times of that in manual procedure and the difference of cell number in a 100 mL vessel was estimated to be about  $4 \times 10^7$  cells in a single run. Therefore, high efficient dissociation strategies using the suitable non-manual device might contribute to reducing the cost for producing cells.

Manual cell aggregate dissociating procedure is also based on the shear stress in pipetting, but the suitable shear stress levels to dissociate cell aggregates remained unclear. As shown in Fig. 4, isolating cell efficacy by using  $\phi 22\text{mm}$  and  $\phi 25\text{mm}$  devices at 1200 rpm was inferior to that with manual procedure and  $\phi 28\text{mm}$  device procedure at 1200 rpm in 771–2 cell line. Since shear stress in  $\phi 28\text{mm}$  device at 1200 rpm was around 2.0 Pa and that in  $\phi 22\text{mm}$  and  $\phi 25\text{mm}$  devices at 1200 rpm was between 0.6 and

1.2 Pa (Fig. 3), shear stress around 2.0 Pa might be necessary for dissociating cell aggregates of 771–2 iPSC. On the other hand, cell aggregates of Ff-I14 were sufficiently dissociated with manual procedure and device procedure at 1200 rpm except for with the  $\phi$ 22mm device. Shear stress in the  $\phi$ 22mm device at 1200 rpm was between 0.6 and 0.8 Pa, while that in  $\phi$ 25mm device at 1200 rpm was between 0.6 and 1.2 Pa. Therefore, at least over 0.8 Pa might be necessary for dissociating Ff-I14-derived undifferentiated cell aggregates. We applied the  $\phi$ 28mm device procedure at 1500 rpm for dissociating cell aggregates after the cardiac differentiation of Ff-I14 iPSC. High shear stress around 2.0 Pa in the  $\phi$ 28mm device procedure at 1500 rpm is sufficient to isolate cardiomyocytes without affecting cardiomyocyte viability. Although the adequate shear stress levels might be different among cell lines and culture conditions, the quantification of shear stress data in the present study might be useful for estimating the suitable shear stress levels for dissociating cell aggregates.

It is well known that Taylor-Couette flow generates various types of flow regimes including Couette flow, Taylor vortex flow, wavy vortex flow, modulated wavy vortex flow, and turbulent flow according to the Reynolds number [19,20]. In the present study, Reynolds number was between 736 and 1609 in  $\phi$ 22mm device, between 758 and 1190 in  $\phi$ 25mm device and between 582 and 1181 in  $\phi$ 28mm device (Fig. 3d). Since it has been reported that turbulent flow is observed when Reynolds number is over around 1400 in the device (Radius ratio = 0.833) [19] and over 2133 in the device (Radius ratio = 0.68) [20], the flow observed in this study might be the wavy or modulated vortex flow.

Furthermore, efficient dissociation of cell aggregates might be useful to reduce the risk of remaining undifferentiated iPSC in the regenerative medicine products. Lin 28 expression analysis is widely used to evaluate the remaining iPSC in cells for transplantation [21] and some strategies that induce iPSC cell apoptosis have reported to reduce Lin28 expression levels in bioengineered tissues and prevent tumor formation [22]. As shown in Fig. 5f, Lin28 expression levels in cells after the device procedure was significantly low compared with levels produced by manual procedure after 4 days in culture. There are some possible explanations for this result. Since PSC are known to easily die while in single cell suspension [23,24], efficient dissociation of cell aggregates to single cells might prevent the growth of the remaining iPSC unless cultured on the suitable cell culture substrate such as laminin E8 fragment [25]. Shear stress itself in the  $\phi$ 28mm device at 1500 rpm applied for cell aggregates after the cardiac differentiation might be harmful for iPSC.

A Taylor Couette flow-mediated cell aggregate dissociation device enabled to generate adequate shear stresses and isolation of single cells from cell aggregates during undifferentiated expansion and following cardiac differentiation. Further scale up of devices and understanding the appropriate shear stress levels will contribute to efficient cell production from PSC for regenerative medicine.

#### Author contributions

KM, MW, KS and YM designed and performed the experiments. KM and KS wrote the manuscript. TS supervised the experiments and edited the manuscript. All authors read and approved the final manuscript.

#### Competing financial interest

There is potential competing interest.

Katsuhisa Matsuura, Masanori Wada and Tatsuya Shimizu are inventors of bioreactor systems. Katsuhisa Matsuura, Masanori

Wada, Katsuhisa Sakaguchi and Tatsuya Shimizu are inventors of cell aggregates dissociation device.

#### Acknowledgment

We thank S. Sugiyama, and M. Matsuda for their excellent technical assistance. We thank Prof. Y. Sawa in Osaka University, Japan and Prof. Y. Yoshida in Kyoto University, Japan for the fruitful collaboration for the development of cardiac differentiation protocol. We thank S. Bou-Ghannam for English proofreading of the manuscript. This work was funded by a grant from Projects for Technological Development in Research Center Network for Realization of Regenerative Medicine of the Japan Science and Technology Agency, JST and Japan Agency for Medical Research and Development, AMED (Grant Number JP17bm0404015).

#### Appendix A. Supplementary data

Supplementary data to this article can be found online at <https://doi.org/10.1016/j.reth.2019.04.006>.

#### References

- [1] Haraguchi Y, Matsuura K, Shimizu T, Yamato M, Okano T. Simple suspension culture system of human iPSC cells maintaining their pluripotency for cardiac cell sheet engineering. *J Tissue Eng Regen Med* 2015;9:1363–75.
- [2] Matsuura K, Wada M, Shimizu T, Haraguchi Y, Sato F, Sugiyama K, et al. Creation of human cardiac cell sheets using pluripotent stem cells. *Biochem Biophys Res Commun* 2012;425:321–7.
- [3] Masuda S, Matsuura K, Shimizu T. Preparation of iPSC cell-derived CD31(+) endothelial cells using three-dimensional suspension culture. *Regen Ther* 2018;9:1–9.
- [4] Mihara Y, Matsuura K, Sakamoto Y, Okano T, Kokudo N, Shimizu T. Production of pancreatic progenitor cells from human induced pluripotent stem cells using a three-dimensional suspension bioreactor system. *J Tissue Eng Regen Med* 2017;11:3193–201.
- [5] Pagliuca FW, Millman JR, Gurtler M, Segel M, Van Dervort A, Ryu JH, et al. Generation of functional human pancreatic beta cells in vitro. *Cell* 2014;159:428–39.
- [6] Arauchi A, Matsuura K, Shimizu T, Okano T. Functional thyroid follicular cells differentiation from human-induced pluripotent stem cells in suspension culture. *Front Endocrinol* 2017;8:103.
- [7] Ito Y, Nakamura S, Sugimoto N, Shigemori T, Kato Y, Ohno M, et al. Turbulence activates platelet biogenesis to enable clinical scale ex vivo production. *Cell* 2018;174:636–648 e18.
- [8] Masuda S, Matsuura K, Shimizu T. Inhibition of LYPD1 is critical for endothelial network formation in bioengineered tissue with human cardiac fibroblasts. *Biomaterials* 2018;166:109–21.
- [9] Sasaki D, Matsuura K, Seta H, Haraguchi Y, Okano T, Shimizu T. Contractile force measurement of human induced pluripotent stem cell-derived cardiac cell sheet-tissue. *PLoS One* 2018;13:e0198026.
- [10] Lee S, Sasaki D, Kim D, Mori M, Yokota T, Lee H, et al. Ultrasoft electronics to monitor dynamically pulsing cardiomyocytes. *Nat Nanotechnol* 2019;14:156–60.
- [11] Seta H, Matsuura K, Sekine H, Yamazaki K, Shimizu T. Tubular cardiac tissues derived from human induced pluripotent stem cells generate pulse pressure in vivo. *Sci Rep* 2017;7:45499.
- [12] Ishida M, Miyagawa S, Saito A, Fukushima S, Harada A, Ito E, et al. Transplantation of human-induced pluripotent stem cell-derived cardiomyocytes is superior to somatic stem cell therapy for restoring cardiac function and oxygen consumption in a porcine model of myocardial infarction. *Transplantation* 2019;103:291–8.
- [13] Matsuhashi Y, Sameshima K, Yamamoto Y, Umezumi M, Iwasaki K. Investigation of the influence of fluid dynamics on thrombus growth at the interface between a connector and tube. *J Artif Organs* 2017;20:293–302.
- [14] Nakagawa M, Taniguchi Y, Senda S, Takizawa N, Ichisaka T, Asano K, et al. A novel efficient feeder-free culture system for the derivation of human induced pluripotent stem cells. *Sci Rep* 2014;4:3594.
- [15] Matsuura K, Kodama F, Sugiyama K, Shimizu T, Hagiwara N, Okano T. Elimination of remaining undifferentiated induced pluripotent stem cells in the process of human cardiac cell sheet fabrication using a methionine-free culture condition. *Tissue Eng C Methods* 2015;21:330–8.
- [16] Zweigert R, Olmer R, Singh H, Haverich A, Martin U. Scalable expansion of human pluripotent stem cells in suspension culture. *Nat Protoc* 2011;6:689–700.
- [17] Yabe SG, Fukuda S, Nishida J, Takeda F, Nashiro K, Okochi H. Induction of functional islet-like cells from human iPSC cells by suspension culture. *Regen Ther* 2019;10:69–76.

- [18] Nath SC, Tokura T, Kim MH, Kino-oka M. Botulinum hemagglutinin-mediated in situ break-up of human induced pluripotent stem cell aggregates for high-density suspension culture. *Biotechnol Bioeng* 2018;115:910–20.
- [19] Grossmann S, Lohse D, Sun C. High-Reynolds number Taylor-Couette turbulence. *Annu Rev Fluid Mech* 2016;48:53–80.
- [20] Nemri M, Climent E, Charton S, Lanoe J-Y, Ode D. Experimental and numerical investigation on mixing and axial dispersion in Taylor-Couette flow patterns. *Chem Eng Res Des* December 2013;91(12):2346–54.
- [21] Kuroda T, Yasuda S, Kusakawa S, Hirata N, Kanda Y, Suzuki K, et al. Highly sensitive in vitro methods for detection of residual undifferentiated cells in retinal pigment epithelial cells derived from human iPS cells. *PLoS One* 2012;7:e37342.
- [22] Matsuura K, Ito K, Shiraki N, Kume S, Hagiwara N, Shimizu T. Induced pluripotent stem cell elimination in a cell sheet by methionine-free and 42 degrees C condition for tumor prevention. *Tissue Eng C Methods* 2018;24:605–15.
- [23] Amit M, Carpenter MK, Inokuma MS, Chiu CP, Harris CP, Waknitz MA, et al. Clonally derived human embryonic stem cell lines maintain pluripotency and proliferative potential for prolonged periods of culture. *Dev Biol* 2000;227:271–8.
- [24] Watanabe K, Ueno M, Kamiya D, Nishiyama A, Matsumura M, Wataya T, et al. A ROCK inhibitor permits survival of dissociated human embryonic stem cells. *Nat Biotechnol* 2007;25:681–6.
- [25] Miyazaki T, Futaki S, Suemori H, Taniguchi Y, Yamada M, Kawasaki M, et al. Laminin E8 fragments support efficient adhesion and expansion of dissociated human pluripotent stem cells. *Nat Commun* 2012;3:1236.